

## ORGANIC RADICALS IN NATURAL APATITES ACCORDING TO EPR DATA: POTENTIAL GENETIC AND PALEOCLIMATIC INDICATORS

L. G. Gilinskaya

UDC 549.753.1: 548.737:538.113:535.34

In a group of natural marine apatites  $\text{Ca}_5(\text{PO}_4)_3(\text{F}, \text{OH})$ , organic  $\dot{\text{C}}\text{H}_3$ ,  $\dot{\text{C}}\text{H}_2\text{-R}$ ,  $\text{HO}\dot{\text{C}}\text{HR}$ ,  $(\text{CH}_3)_2\dot{\text{C}}\text{R}$ , and  $-\dot{\text{C}}_{\text{org}}$  radicals are identified by EPR. The relation between the EPR spectra of the observed organic radicals, the valence form, and the structural location of impurity vanadium ions ( $\text{V}^{4+}$  ( $\text{VO}^{2+}$ ) on the  $\text{Ca}^{2+}$  II site or  $\text{V}^{5+}$  ( $\text{VO}_4$ ) $^{3-} \rightarrow (\text{PO}_4)$  $^{3-}$ ) is established. The structure of organic radicals correlates with the type of organic matter in the sample under analysis: sapropelic or humic, depending on the climatic conditions of mineral genesis.

**Keywords:** organic radicals, vanadyl ion complexes, EPR spectra, natural marine apatites, paleoclimate.

### INTRODUCTION

Organic matter is a companion of all geological processes that are mostly long-lasting and multi-parameter. Inclusions of carbon-bearing matter (non-carbonate carbon) of different origin in minerals and rocks have been actively studied by different methods, but a special place belongs to the electron paramagnetic resonance (EPR) or electron spin resonance (ESR), advantages of which and the uniqueness of information obtained by this method are adequately covered in the literature [1-4]. The ESP spectra of various types (forms) of organic radicals (ORs) in solutions and solid states have been much studied in all aspects in chemistry of organic compounds [5, 6]. In minerals and their synthetic analogues, in different natural objects, only singular OR types with characteristic ESP spectra have been described. Most often, the literature describes the  $\dot{\text{C}}\text{H}_3$  [2, 6-8],  $\dot{\text{C}}\text{H}_2\text{-COOH}$  [6, 9] radicals and seldom  $(\text{CH}_3)_2\dot{\text{C}}$  [10] and perinaphthenyl [11] ones. For many natural objects the ESP spectrum of OR is represented by a single symmetrical line of different width and intensity determined by an unpaired electron localized on the broken carbon bond in the aromatic ring system, as for instance, in carbonates [12], feldspars [13], peat, coals, bitumen, and oil [4]. Identification of the organic matter, which can be performed based on the analysis of the ESP spectra of OR, is important in order to obtain the genetic data on the formation conditions of natural objects and subsequent superimposed processes.

The presence of organic matter (OM) in apatite is predetermined by the very nature of the polygenic mineral. This mineral is present in living organism (tooth enamel, bones, pathogenic formations on cardiac valves, in the kidneys, gallbladder, artificial implants) involved in metabolic processes, i.e. it is on the borderline between living and non-living matter. ORs are logically expectable in the biological varieties of apatite, which has been confirmed by numerous studies.

Experiments proved the formation of inorganic apatite from organic phosphorus [14]. The formation of marine, the so-called primary sedimentary apatites is associated with biogenic [15] and bacterial [16] activity.

The ability of apatite to interact with organic substances, to absorb them was noticed as early as 1861, when it was used as sorbent to purify pepsin and later in chromatography in separation of proteins and nucleic acids. It is these special features of apatite that contributed to the development of extensive studies of the absorption of different organic substances by the mineral constituent of teeth and bones [17-19], which is important to prevent dental caries and calculi formation, and also the fixing mechanism for flotation reagents [20]. As a result, the following apatite properties were established: 1) the presence of a highly polarized surface that promotes active interaction with different reagents; the apatite ability to form strong bonds with polar and polarizable molecules was noted; 2) the main absorbing sites are those of Ca and P, where the former bind acid groups and the latter bind basic ones.

The inclusion of organic  $\text{CH}_2\text{-COO}$  molecules [21] in the channels of the apatite structure, the absorption of organic phosphates and polyphosphonates by the surface [22, 23] were established by IR spectroscopy. The investigation of tooth enamel using the electron spectroscopy showed that it contains OM in the form of strings within the enamel crystals [24]. Using EPR, the  $\dot{\text{C}}\text{H}_3$  and  $\dot{\text{C}}\text{H}_2\text{-OH}$  radicals were detected in irradiated synthetic apatites [7, 9], and  $(\text{CH}_3)_2\text{-}\dot{\text{C}}\text{R}$  was found in human tooth enamel and other bioapatites irradiated and then heated in the nitrogen gas flow to  $T$  of 400 K [10].

We have previously reported on ORs in the structure of natural and synthetic apatites of sedimentary genesis. For the first time, in the inorganic matrix the formyl radical  $\dot{\text{H}}\text{CO}$  was detected by EPR, the intensity of which correlated with nonstoichiometry of the apatite composition, the Ca/P ratio (the stoichiometry ratio  $\text{Ca/P} = 1.67$ ) [25, 26]. In the samples with  $\text{Ca/P} > 1.67$ , the  $\dot{\text{H}}\text{CO}$  radical was observed, and in the samples with  $\text{Ca/P} < 1.67$ , the spectrum of  $\text{H}^0$  atomic hydrogen was recorded indicating the presence of  $\text{HPO}_4^{2-}$  acid groups in the structure [27, 28]. In catagenetically transformed apatites of the marine and supergene genesis, by means of EPR we identified the organophosphorus radicals with the specific  $^{31}\text{P}$  splitting: phosphinyl- $\text{P}(\text{OR})_2$ , phosphoryl- $\text{P}(\text{OR})_3$ , and phosphoranyl- $\text{P}(\text{OR})_4$  ( $\text{R} = \text{CH}_2, \text{CH}_3$  or  $\text{C}_2\text{H}_5$ ) [29]. This means that apatite is the only natural mineral, in which due to its structural features, composition, and genesis variations the presence of ORs is quite explicable. This fact bears important structural and genetic information, as the studies performed so far show.

The present paper reports the results of the study of the specific group of this mineral, namely the primary sedimentary apatites, unaltered, the so-called marine apatites, according to the accepted classification. Using thermal analysis, it was determined that they contain OM in the amount of 1-3.5%, and its EPR identification can contribute to the issue of searching typomorphic features of this group.

We have previously investigated  $\text{VO}^{2+}$  vanadium complexes in unaltered marine apatites, granular and nodular, and have noted their disappearance in catagenetically transformed samples [30]. It was proposed to consider  $\text{VO}^{2+}$  complexes as a typomorphic feature of the marine genesis of apatites. However, not all forms of granular apatites were covered in the first study. With extending the scope of material being studied, a number of questions arose. It appeared that in the samples from some deposits of marine genesis,  $\text{VO}^{2+}$  complexes were not recorded by EPR in spite of the vanadium presence, according to the analytical data. It was also noted that  $\text{VO}^{2+}$  complexes were accompanied by the spectra not identified previously in natural apatites. In order to clarify these questions the present study was performed.

Close geochemical relation between carbonic (organic) matter and all naturally occurring processes of mineral formation with subsequent transformations raises it to the rank of significant information parameter not only in geological genetics, but also in paleoclimatic reconstructions because changes in the climate (temperature, humidity) affects flora and fauna that underlie OM. In selecting material, we took into account such a parameter as the geological age.

## EXPERIMENTAL

We studied three different age petrographic types of primary marine phosphorite apatites of sedimentary genesis: granular, nodular, and conchoidal. Granular apatites are represented by: *a*) primary phosphate organogenic fossils (bone splinters and tooth fragments of fishes, skate, shark spinal bones and teeth, bony-fish pattern) from Jeroy, Jilga, and Jingoda deposits (Middle Eocene, Upper Paleocene, Cretaceous); *b*) phosphatized primary calcareous fossils of fauna (pelecypods, foraminiferas, gastropods) from Shorbulak, Kyariz, Karakata, Tashkura, and Vodokachka deposits (Eocene); *c*) apatites from the phosphorite deposits of North Western Africa and America (Middle Eocene, Upper Cretaceous, Miocene).

Nodular phosphorite apatites were taken from two deposits of the East European Platform: Polpino (Upper Cretaceous) and Egor'evskoye (Malm–Lower Cretaceous); conchoidal phosphorite apatites were taken from the Baltic deposits (Maardu, Kingisepp). Samples were analyzed using X-ray diffraction technique and IR spectroscopy; thermal analysis was employed to determine the amount of OM in these samples. The analytical data for the most samples studied have been reported in our work [31] on the investigation of carbonate carbon geochemistry in sedimentary apatites. The samples are comprised of FOH and OH varieties of fine, polycrystalline carbonate apatite with a different degree of crystallinity because no single crystals occur in this genetic group in nature.

The EPR spectra were examined at room temperature on a Radiopan SE/X 2544 radiospectrometer ( $\lambda = 3.2$  cm,  $f_{\text{mod}} = 100$  kHz) with a double resonator. The samples were annealed in the air and exposed to synchrotron radiation (SR) from a storage ring VEPP-3 at the LIGA station in the air atmosphere; the dose was 10 Mrad.

## RESULTS AND DISCUSSION

The EPR spectra of marine apatites are showed in Fig. 1. The characteristic spectrum observed in all studied groups is associated with a  $V^{4+}$  ion ( $S = 1/2$ ,  $J_v = 7/2$ ) in the vanadyl form  $VO^{2+}$ . We have previously described this spectrum, determined its parameters and substantiated the localization of  $VO^{2+}$  complexes in the Ca(II) site in the apatite structure [30]. The  $VO^{2+}$  spectrum was observed in marine native apatites of different geological age, but in catagenetically transformed samples ( $T$  300°C, pressure 2500-3000 kg/cm<sup>2</sup>) it was absent. Subsequent researches confirmed the conclusion that vanadium gets out of structure in catagenesis [32].

The analysis of EPR spectra of vanadyl in a wider range of natural apatites presented in this study made it possible to identify some patterns.

I. In the group of granular apatites, the  $VO^{2+}$  spectrum is recorded in all cases and is particularly intense and distinct in the phosphorite apatites from Africa and America (Fig. 1 (1), subgroup *c*). In other subgroups (*a*, *b*), the spectrum intensity is highly variable, and in some samples (Fig. 1 (2), subgroup *a*) it drops even to trace amounts. In marine apatites of another morphological form (nodular), the spectrum is not always observed. For examination, the samples of phosphorite apatites from two of the East European Platform deposits were taken: Polpino and Egor'evskoye. Only in the most Polpino samples, the  $VO^{2+}$  spectrum is recorded (Fig. 1 (1)), whereas in all samples from the Egor'evskoye deposit, it is absent (Fig. 1 (3)).

II. The  $VO^{2+}$  spectrum is **always** accompanied by additional lines located between lines 4 and 5 of  $H \perp z$  orientation in the  $VO^{2+}$  spectrum, as can be seen in Fig. 1 (1), (2). Among these are the intense lines caused by inorganic radicals and relatively weaker ones symmetrically located around  $g_e$ . The inorganic  $CO_2^-$ ,  $CO_3^-$ , and  $CO_3^{3-}$  radicals of carbonate carbon we have studied in detail in supergene apatites, where the organic radicals are absent and do not complicate the identification [31, 33, 34]. They are observed in all types of natural carbonate apatites.

Figure 2 depicts different (in intensity) variants of the spectra of other relatively weaker lines from the central part of the total spectra. The analysis shows that the spectra stem from the organic  $\dot{C}H_3$  and  $\dot{C}H_2-R$  radicals, whose reliably identifiable parameters are given in Table 1 and which well agree with those previously obtained for synthetic apatites [9]. The spectrum of the third radical appeared to be the least intense of them (Fig. 2 (2)), which was permanently recorded

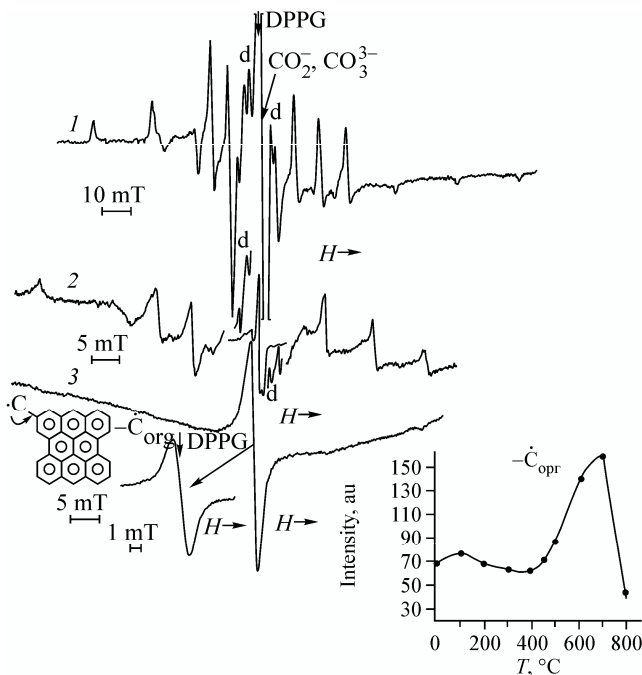


**Fig. 1.** EPR spectra of natural granular (1), (2) and nodular (3) apatites. The central part of the spectrum is recorded with lower gain. Hereinafter DPPG is a position of the reference signal of diphenylpicrylhydrazyl; *d* are the additional lines in the spectrum of the  $\text{VO}^{2+}$  ion between 4 and 5 with  $H \perp z$  orientation.

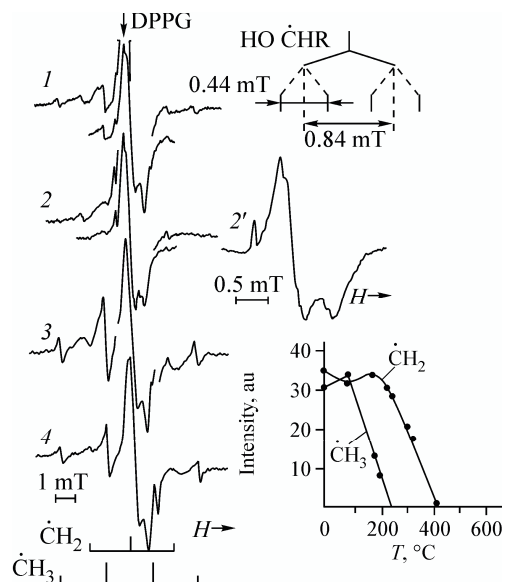


**Fig. 2.** Spectra of the organic  $\dot{\text{C}}\text{H}_3$ ,  $\dot{\text{C}}\text{H}_2\text{-R}$ ,  $\text{HO}\dot{\text{C}}\text{HR}$  radicals in granular apatites; the central part of the total spectra shown in Fig. 1. Spectra of samples with different geological age: 1, 2, 2' Eocene (Jilga), 3, 4 Cretaceous period (Jingoda). Lines from inorganic radicals of carbonate carbon on spectra 1 and 3 recorded with lower gain.

**TABLE 1.** Parameters of the Spin Hamiltonian of Organic Radicals in Natural Apatites

Radical	$A$ , mT	$g$ factor	Radical	$A$ , mT	$g$ factor
$\dot{\text{C}}\text{H}_2\text{-R}$	2.09	2.0022	$(\text{CH}_3)_2\text{-}\dot{\text{C}}\text{R}$	2.15	2.0024
$\dot{\text{C}}\text{H}_3$	2.24	2.0018	$^*\text{VO}^{2+}$	$A_z = 19.1$	$g_z = 1.930$
$\text{HO}\dot{\text{C}}\text{HR}$	$A_{\text{H1}} = 0.84$ $A_{\text{H2}} = 0.44$	2.0008		$A_x = 7.2$	$g_x = 1.975$
$\dot{\text{C}}_{\text{org}}$		2.0025		$A_y = 6.3$	$g_y = 1.971$
				$A_0 = 10.86$	$g_0 = 1.956$

\*Data from [30]. For the  $\text{VO}^{2+}$  ion, the determination accuracy of parameter components is  $A \pm 0.1$  mT,  $g$  factor  $\pm 0.001$ ; for organic radicals,  $A \pm 0.03$  mT,  $g$  factor  $\pm 0.0005$ .

together with the above. Its noticeable presence in the samples is accomplished by their black color. The analysis was complicated by transposition with the spectrum of inorganic radicals of carbonate carbon. Based on a comparison of the observed spectrum pattern and the hyperfine splitting values with the data provided in the work [2], the spectrum was supposed to be determined by the  $\text{HO}\dot{\text{C}}\text{HR}$  radical with splitting into two nonequivalent hydrogen atoms (Fig. 2 (2), (2')).

Note that the spectra of  $\dot{\text{C}}\text{H}_3$ ,  $\dot{\text{C}}\text{H}_2\text{-R}$  radicals in the samples of Cretaceous age (ancient) appeared to be most distinct, in which the  $\text{VO}^{2+}$  spectrum was absent (Fig. 2 (3), (4)). The analysis of radical thermal behavior presented in the

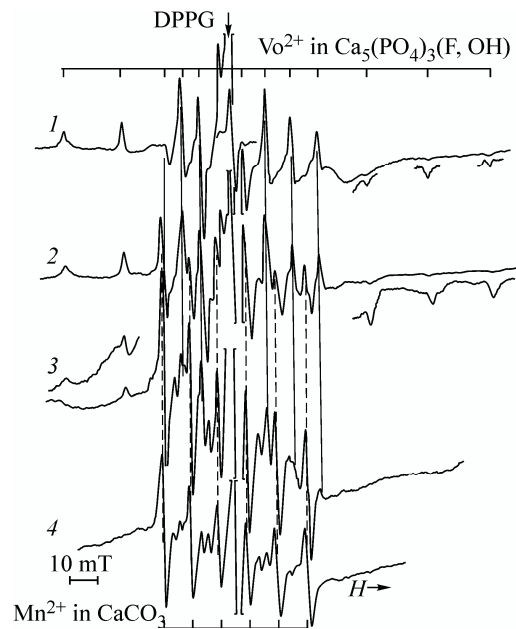


**Fig. 3.** EPR spectra of  $\text{VO}^{2+}$  complexes in  $\text{Ca}_5(\text{PO}_4)_3(\text{F}, \text{OH})$  and  $\text{Mn}^{2+}$  in  $\text{CaCO}_3$  observed in the subgroup *b* (phosphatized invertebrates) of granular apatites with difference intensity ratio: (1) pure spectrum of  $\text{VO}^{2+}$ , (2)  $\text{VO}^{2+} > \text{Mn}^{2+}$ , (3)  $\text{VO}^{2+} < \text{Mn}^{2+}$ , (4) pure spectrum of  $\text{Mn}^{2+}$  in  $\text{CaCO}_3$ . Spectra of  $\text{VO}^{2+}$  and  $\text{Mn}^{2+}$  denoted by solid and dashed lines respectively.

same figure showed a higher stability of the  $\dot{\text{C}}\text{H}_2\text{-R}$  radical as compared with  $\dot{\text{C}}\text{H}_3$ . These three organic radicals together always accompany the spectrum of the vanadyl ion, correlate with it in intensity and are observed in non-irradiated natural samples. No marked effect of additional irradiation on the spectrum intensity of the organic radicals is detected.

In the samples of nodular apatites, where the spectrum of  $\text{VO}^{2+}$  is not recorded (part of samples from the Polpino deposit, all samples from Egor'evskoye), a single symmetrical line is observed in the  $g_e$  area with  $\Delta H_{\text{Pol}} = 1.15$  mT and  $\Delta H_{\text{Eg}} = 1.3$  mT (Fig. 1 (3)). The kinetic curve of thermal annealing of the center is given in Fig. 1 (3) for a sample from the Egor'evskoye deposit. The second sample showed a similar curve differing only in the maximum intensity temperature:  $T_{\text{Pol}} 600^\circ$  as compared with  $T_{\text{Eg}} 700^\circ\text{C}$  for the previous sample. The center is determined by the organic carbon radical, similar to that observed in peat, coals, bitumen, and other natural objects, as mentioned above, with an unpaired electron on the broken carbon bond stabilized by a system of aromatic rings (denoted as  $-\dot{\text{C}}_{\text{org}}$ ). The differences in the line widths as well as in the maximum intensity temperatures of annealing appear to indicate a minor difference in the composition of OM.

In the subgroup *b* of granular apatites (phosphatized fossils of fauna), spectra of  $\text{VO}^{2+}$  in the apatite structure and of  $\text{Mn}^{2+}$  in  $\text{CaCO}_3$  are observed simultaneously in most samples, i.e. the fossils of primary calcareous mollusk shells are manifested (Fig. 3). The ratio between them in samples taken from different places of the same deposit varies from the pure spectrum of  $\text{VO}^{2+}$  (Fig. 3 (1)) to the pure spectrum of  $\text{Mn}^{2+}$  in  $\text{CaCO}_3$  (Fig. 3 (4)) through intermediate variants (Fig. 3 (2), (3)); therewith, they are also accompanied by different organic radicals: the  $\dot{\text{C}}\text{H}_3$ ,  $\dot{\text{C}}\text{H}_2\text{-R}$  group and  $\text{HO}\dot{\text{C}}\text{HR}$  along with  $-\dot{\text{C}}_{\text{org}}$  respectively.

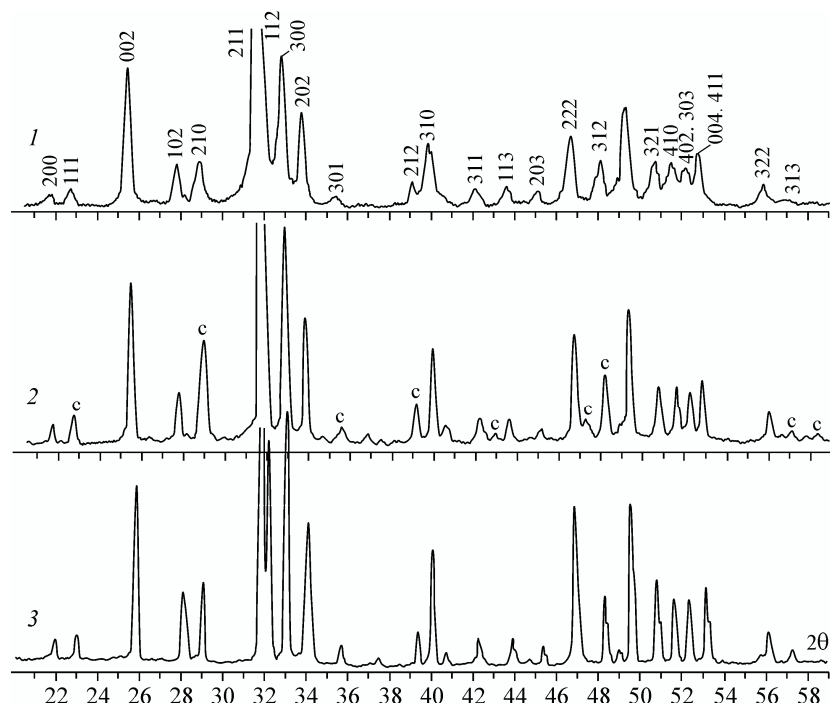


**Fig. 4.** X-ray diffraction pattern of granular (1), (2), subgroup (b) and nodular (3) apatites.

Initially, it was supposed that the EPR spectra record the process of apatite substitution for calcite, and using computer modeling, it is possible to obtain the quantitative ratio between them. However, according to the X-ray data, it appeared that all samples were presented by apatite with a very small fraction of calcite in some of them. In Fig. 4, the X-ray diagrams (1), (2) of samples with pure spectra of  $\text{VO}^{2+}$  (3 (1)) and  $\text{Mn}^{2+}$  (3 (4)) respectively are given. The calcite peaks in the X-ray patterns (c) represent a very small addition to the apatite peaks. The general view of X-ray patterns gives evidence of poor crystallinity of the subgroup under study as compared with phosphorite apatites (Fig. 4 (3), subgroup c).

The absence of the EPR spectrum of vanadyl in some samples, a change in the intensity within one deposit, and the manifestation of different-type organic radicals are likely to have the same cause as in the group of nodular apatites. The cause is that the samples contain OM of different types: sapropelic (aliphatic) and humic (aromatic) corresponding to different conditions of the apatite formation.

The correlation of  $\text{VO}^{2+}$  and OR spectra allows us to believe  $\text{V}^{4+}$  ( $\text{VO}^{2+}$ ) to enter into the apatite structure as organic complexes. It is known that the vanadyl ion exhibits an exceptional affinity for OM forming the  $\text{V}_{\text{org}}$  formula, for example, vanadium petroporphyrin or complexes with phenolic groups in the lignin derivatives [35]. Depending on the oxidation-reduction environment of mineral formation and PH values, vanadium is in different valence forms:  $\text{V}^{3+}$ ,  $\text{V}^{4+}$ , and  $\text{V}^{5+}$ . The vanadyl ion  $\text{VO}^{2+}$  ( $\text{V}^{4+}$ ), as can be seen from the literature and our experimental data, seem to form complexes with aliphatic organics, as judged from the types of the observed radicals in the group of granular apatites. The complexes are very stable. The analysis of thermal annealing kinetic curves for the spectrum of vanadium shows that its intensity remains almost unchanged up to  $T$  400°C. The spectrum disappears in a range of  $T$  450-600°C depending on the sample composition. In the group of nodular apatites, humic (aromatic) organics predominate, and vanadium is likely to be in the  $\text{V}^{5+}$  state substituting for phosphorus:  $(\text{VO}_4)^{3-} \rightarrow (\text{PO}_4)^{3-}$ . In the EPR spectra of these samples, only the  $-\dot{\text{C}}_{\text{org}}$  radical is manifested.

The difference in the composition of OM in two different morphological types of marine apatites is also indicated by the thermal analysis data. In granular apatites, OM is burnt at  $T$  320-360°C, and in nodular, at  $T$  440-480°C, as we found previously [31]. In addition, researches have demonstrated that nodular apatites from the Egor'evskoye deposit, in which the vanadium content is even higher (75-142 g/t) than that in the samples from the Polpino deposit (18-44 g/t) [32] (however, the

EPR spectrum of  $\text{VO}^{2+}$  is not observed here), contain humic acids (0.54%), bitumen (0.16%), and residual coal (0.75%) in the amounts exceeding the corresponding values for the other genetically similar deposits [36].

Therefore, the absence of the EPR spectrum of  $\text{VO}^{2+}$  in the samples being studied with the presence of vanadium in them according to the analytical data indicates its presence in the  $\text{V}^{5+}$  state, which is caused by changes in pH of the formation environment and in other parameters under the climate effect during the Earth's evolution accompanied by a change in OM (flora and fauna).

The analysis of literature data on the geological and geochemical formation environments of the studied samples shows that the deposits of granular apatites are characteristic of the territories with the arid climate ( $T$  20–22°C, precipitation 500–700 mm/year, tropical, variably humid climate) when sapropelic organics predominate. These are phosphorus-rich ( $\text{P}_2\text{O}_5 > 35\%$ ) apatites. The deposits of nodular apatites belong to the areas with humid climate, where humic organics predominate ( $T$  12–14°C, uniformly humid, relatively cool climate); the phosphorus content is substantially lower ( $\text{P}_2\text{O}_5 = 20\text{--}25\%$ ) in these deposits. The difference in phosphorus concentration between arid and humid areas lies in the intensification of phosphorite accumulation [37]. First of all, its rate seems to change. The lithological type of apatites, grain (from 0.1–0.2 mm to 3 mm) and nodule (from 0.5 cm to 5 cm) sizes [38] as well as the OM type strictly and regularly correspond to the climate conditions of their formation.

Note that, apart from the described above paramagnetic centers, the spectrum of a structural impurity  $\text{Fe}^{3+}$  ion ( $g = 4.27$ ) is recorded in the studied samples, which has substantially higher intensity in granular apatites as compared to nodular ones. The analysis of iron role in authigenic mineral formation shows that under oxidizing conditions (arid climate) trivalent iron predominates, and under reducing conditions (humid climate) the leading role belongs to divalent iron [37]. The spectra of  $\text{F}^-\text{O}^-\text{F}^-$  and  $\text{OH}^-\text{O}^-$ , the most abundant centers in natural apatites, determined by the entrance of the oxygen structure in the  $\text{O}^-$  form ( $S = 1/2$ ) on the  $6_3$  axis, are very weak and more often are absent both in nodular and granular samples, whereas in marine conchoidal apatites they are already intense.

An interesting feature of the described spectra related to the geological age of apatites being studied was noticed in the analysis of the subgroup (*a*) of granular apatites represented by primary phosphate organogenic fossils (shark teeth, bones, part of bony-fish pattern, spinal bones). In younger samples (Eocene, Upper Paleocene), the spectra of  $\text{VO}^{2+}$  characteristic of the granular group are recorded with the accompanying organic  $\dot{\text{C}}\text{H}_3$ ,  $\dot{\text{C}}\text{H}_2\text{-R}$ , and  $\text{HO}\dot{\text{C}}\text{HR}$  radicals (Fig. 1 (2)). In older (Cretaceous) age apatites (ancient shark teeth), the spectrum of  $\text{VO}^{2+}$  is not observed, but at the same time, the spectra of radicals are recorded, and they have narrower and more intense lines providing the reliable interpretation (Fig. 2 (3) and 2 (4)). Such a situation appears to be reasonably explained by the older age of Cretaceous apatites allowing for their transformation (destruction of vanadyl complexes) as a result of superimposed naturally occurring processes. A comparison of the types and intensities of the observed EPR centers in the studied groups of marine apatites distinguished by their geological age suggests that in formation parameters, including climate, the Cainozoic era (Eocene, Paleocene) was more favorable for the processes of phosphorite formation than the Mesozoic (Cretaceous, Jura).

No less remarkable fact is the spectrum characteristic of the  $(\text{CH}_3)_2\text{-}\dot{\text{C}}\text{R}$  radical, which consisted of seven lines, recorded in some ancient (Cretaceous) apatites (shark teeth) (Fig. 5). The spectrum was reliably identified, though the lines were wide, which may be related to a low degree of crystallinity in the sample.

This spectrum was for the first time obtained in human tooth enamel and other bioapatites (dentine, bird eggshell, steer bones) preliminary irradiated and recorded in the nitrogen flow at  $T$  400 K [10]. The theoretical ratio between the spectrum line intensities of this radical forms a set of numbers: 1:6:15:20:15:6:1.

In our study, we have examined two bioapatites: tooth enamel of an adult person and pathogenic formation on human cardiac valves (cardiolite) that we previously investigated in detail [39–41]. The spectra of these samples, first irradiated and then heated in the air, are shown in Fig. 5. At  $T$  100°C, weak spectra of  $\dot{\text{C}}\text{H}_3$  and  $\dot{\text{C}}\text{H}_2\text{-R}$  radicals first appear,

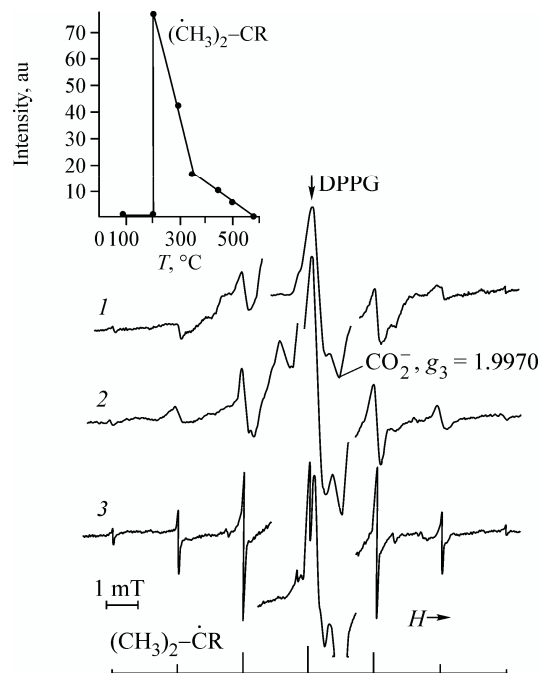


**Fig. 5.** EPR spectra of the  $(\text{CH}_3)_2\dot{\text{C}}\text{R}$  radical in natural and biological apatites: (1) ancient shark tooth (Cretaceous period), (2) cardiolite, pathogenic formation on the human cardiac valve, (3) tooth enamel of an adult person. The central part of the spectrum is recorded with lower gain. The fiducial peak ( $g_3 = 1.9970$ ) of the inorganic  $\text{CO}_2^-$  radical of carbonate carbon is denoted. In the upper left corner of the figure the temperature dependence of the radical spectrum intensity in cardiolite is given.

and at  $T 200^\circ\text{C}$  the  $(\text{CH}_3)_2\dot{\text{C}}\text{R}$  radical appears. In tooth enamel (Fig. 5 (3)), the lines are narrow and their intensity ratio matches with the theoretical set. In cardiolite (Fig. 5 (2)), the spectrum is similar to that of the studied natural sample. The observed difference in the spectra of enamel and cardiolite results from the difference in the degree of crystallinity, as the X-ray diffraction study shows, which confirms the made suggestion that explains the spectrum of the natural sample. The analysis of thermal behavior of this radical, given in the same figure, indicates its stability up to  $T 550^\circ\text{C}$ .

The spectrum of the  $(\text{CH}_3)_2\dot{\text{C}}\text{R}$  radical observed in the natural sample not subjected to any experiments under laboratory conditions unambiguously gives evidence of the presence of radiation and temperature exposure in its history.

Therefore, our research shows that in the complex natural formation (apatite) a large collection of organic radicals is stabilized, which distinguish in nature induced by irradiation or temperature and have different ranges of thermal stability. The relation between the radicals and other paramagnetic centers is determined. As the most organic radicals investigated so far are the derivatives of organic acids, it can be thought that the types identified in this work reflect the geological and geochemical conditions of apatite formation and give reliable evidence of particular substantial differences.

The presence of vanadium in apatite of marine genesis is a typomorphic feature. Sea water is a source of vanadium and OM, composition of which is affected by climate conditions. The form, in which vanadium enters into the apatite structure as  $\text{V}^{4+}$  or  $\text{V}^{5+}$  on different structural sites ( $\text{Ca}^{2+}(\text{II})$  and  $(\text{PO}_4)^{3-}$ ) appeared to be associated with the type of OM, which is indicated by the relation between the spectrum of the  $\text{VO}^{2+}$  vanadyl ion and aliphatic organic radicals examined in



this work. According to the analytical data, the absence of the spectrum of the vanadyl ion in the presence of vanadium correlates with the organic radical of another nature, namely  $-\dot{C}_{\text{org}}$ .

Record of the organic radicals of different structures, association with the type of OM, sensitivity to superimposed naturally occurring processes, notably a change in their concentration (intensity of the EPR spectra) with the geological age and climate, made it possible to explain and answer the existing questions concerning the substantiation of typomorphism of  $\text{VO}^{2+}$  complexes. However, the real model of organic complex with the vanadyl ion in apatite remains to be determined. Further investigations are required involving the extraction of OM from natural apatites, which is contained here in minor amounts. A comparative analysis of parameters of the EPR spectrum of organic complexes with the  $\text{VO}^{2+}$  vanadyl ion in different solids is not yet applicable because now we have only the data on their studies in solutions [42]. We think the results on the types of organic radicals detected in natural apatites obtained in this work can guide the researches in this direction.

We believe not only the analysis of the OR structure in apatite to be of interest, but also their relationship with other existing paramagnetic centers: impurity ions and inorganic radicals. In the present work, the existence of, so to say, parafectiveness (by analogy with paragenesis of minerals) is shown to occur: association of the centers observed in minerals characterizing the genetic parameters and explaining the features of the observed EPR spectra. A clear relation is established between the spectra of  $\text{VO}^{2+}$  and organic  $\dot{\text{C}}\text{H}_3$ ,  $\dot{\text{C}}\text{H}_2\text{-R}$ ,  $\text{HO}\dot{\text{C}}\text{HR}$  radicals, and also the spectrum of  $\text{Fe}^{3+}$  ions, along with the absence of  $\text{O}^-$  paramagnetic oxygen complexes that are almost always present in natural apatites. It is just the analysis of associations of paramagnetic centers in minerals that results in successful application of the method to geological researches.

New organic radicals identified in natural apatites, the relationships of paramagnetic centers established in the work will apparently have the practical use in geological and geochemical researches and will serve as a basis for the solution of theoretical issues in chemistry of coordination compounds and radiospectroscopy. Application of the obtained results to the analysis of specific materials with the detailed geological data will be the subject of a separate publication.

## CONSLUSIONS

1. New organic radicals are identified in non-irradiated natural sedimentary apatites of marine genesis with characteristic EPR spectra:  $\dot{\text{C}}\text{H}_3$ ,  $\dot{\text{C}}\text{H}_2\text{-R}$ ,  $\text{HO}\dot{\text{C}}\text{HR}$ ,  $(\text{CH}_3)_2\text{-}\dot{\text{C}}\text{R}$ , and  $\dot{C}_{\text{org}}$ .

2. Spectra of the  $\text{VO}^{2+}$  vanadyl ion and  $\dot{\text{C}}\text{H}_3$ ,  $\dot{\text{C}}\text{H}_2\text{-R}$ ,  $\text{HO}\dot{\text{C}}\text{HR}$  radicals always manifest themselves together, which indicates the entrance of vanadium into the structure on the  $\text{Ca}^{2+}(\text{II})$  site in the form of stable organic complexes that can be called typomorphic for marine apatites formed in the arid climate.

3. The analysis of  $(\text{CH}_3)_2\text{-}\dot{\text{C}}\text{R}$  nature performed under laboratory conditions made it possible to state that its presence in ancient (Cretaceous) apatites evidences radiation and temperature exposure in their geological history.

4. The relation is found between the structure of organic radicals (aliphatic and aromatic) and the type of OM in the sample (sapropelic or humic) corresponding to different climate conditions of mineral formation.

5. The ratio between the spectra of  $\text{VO}^{2+}$  in association with organic radicals in  $\text{Ca}_5(\text{PO}_4)_3(\text{F},\text{OH})$  and  $\text{Mn}^{2+}$  in  $\text{CaCO}_3$  in phosphatized primary calcareous fossils of fauna (foraminiferas, pelecypodas, etc.) can be used as indication of changes in climate conditions of the mineral formation environment.

I deem it my pleasant duty to express my sincere thanks to Profs. Yu. N. Zanin and R. G. Knubovets for providing samples for the study, to Dr. T. N. Grigor'eva for performing X-ray diffraction analysis, and to Dr. L. I. Razvorotneva for helpful consultations.

The work was supported by RFBR project No. 08-05-64680.

## REFERENCES

1. D. J. E. Ingram, *Biological and Biochemical Applications of Electron Spin Resonance*, X und 311 Seiten, Adam Hilger Ltd., London (1969).
2. J. Vertz and J. Bolton, *Electron Spin Resonance, Elementary Theory and Practical Applications*, McGraw-Hill Book Company, New York (1972).
3. I. V. Matyash, A. B. Brik, A. P. Zayatz, and V. V. Mazykin, *Radiospectroscopy of Quartz* [in Russian], Naukova Dumka, Kiev (1987).
4. B. F. Alekseev, A. M. Belonogov, Yu. V. Bogachev, et al., *Magnetic Resonance in the Study of Natural Formations* [in Russian], Nedra, Leningrad (1987).
5. S. Ya. Pshcheshetskii, A. G. Kotov, V. K. Milinchuk, et al., *EPR of Free Radicals in Radiation Chemistry* [in Russian], Khimiya, Moscow (1972).
6. A. L. Buchachenko and A. M. Vasserman, *Stable Radicals: Electronic Structure, Reactivity, and Application* [in Russian], Khimiya, Moscow (1973).
7. G. Bacquet and V. O. Quang Truong, *J. Sol. St. Chem.*, **39**, 148 (1981).
8. I. V. Matyash, A. B. Brik, S. A. Galii, et al., *Geokhimiya*, No. 6, 916 (1983).
9. H. Ishii and M. Ikeya, *Appl. Radiat. Isotop.*, **44**, 95 (1993).
10. A. Roufosse, L. J. Richelle, and O. R. Gilliam, *Archs oral Biol.*, **21**, 227 (1976).
11. H. Chandra, M. C. R. Symons, and D. R. G. Griffiths, *Nature*, **332**, 526 (1988).
12. F. A. Murav'ev, V. M. Vinokurov, A. A. Galeev, et al., *Georesursy*, **2** (19), 40 (2006).
13. I. V. Matyash, A. S. Litovchenko, N. N. Bagmut, et al., *Radiospectroscopy of Feldspars* [in Russian], Naukova Dumka, Kiev (1981).
14. J. Lucas and L. Prevot, *C.R. Acad. Sci. (Paris)*, Ser. II, **292**, 1203 (1981).
15. N. V. Shabanina, *Litol. i Polezn. Isk.*, No. 3, 82 (1988).
16. Yu. N. Zanin, *Litosfera*, No. 2, 159 (2005).
17. R. A. Beele and A. S. Posner, *Coll. Intern. C. N. R. S*, No. 230, 275 (1975).
18. G. Bernardi, *ibid*, 463.
19. H. R. Rawls, T. Bartels, and J. Arends, *J. Coll. Interf. Sci.*, **87**, No. 2, 339 (1982).
20. R. G. Knubovetz and B. M. Maslennikov, *Dokl. Akad. Nauk SSSR*, **164**, No. 2, 387 (1965).
21. C. Rey, J. C. Trombe, and G. Montel, *C.R. Acad. Sci. Paris*, **283C**, 465 (1976).
22. H. R. Rawls and J. Calasso, *Adsorption on and Surface Chemistry of Hydroxyapatite*, Plenum Press, New York (1984), p. 115.
23. D. N. Misra, *ibid*, 105.
24. A. Millard and F. G. Pautard, *Vinter Kongress fur Electronenmikroskope*, Springer Verlag, Berlin (1960), Band I, 357.
25. L. G. Gilinskaya and M. V. Chaikina, *Zh. Strukt. Khim.*, **20**, No. 6, 1120 (1979).
26. L. G. Gilinskaya, M. V. Chaikina, and Yu. N. Zanin, *A Study of Calcium Phosphates by Physical Methods* [in Russian], Nauka, Novosibirsk (1979), 94.
27. L. G. Gilinskaya, M. V. Chaikina, and M. Ya. Shcherbakova, *Koordinats. Khim.*, **2**, Vyp. 4, 517 (1976).
28. L. G. Gilinskaya and M. V. Chaikina, *Izv. Akad. Nauk SSSR, Neorg. Mater.*, **13**, No. 3, 577 (1977).
29. L. G. Gilinskaya, Yu. N. Zanin, R. G. Knubovets, et al., *J. Struct. Chem.*, **33**, No. 6, 859-870 (1992).
30. L. G. Gilinskaya and Yu. N. Zanin, *Dokl. Akad. Nauk SSSR*, **273**, No. 6, 1463 (1983).
31. L. G. Gilinskaya, T. N. Grigorieva, Yu. N. Zanin, et al., *Geokhimiya*, No. 3, 279 (2001).
32. Yu. N. Zanin, A. G. Zamirailova, and G. M. Pisareva, *Dokl. Akad. Nauk*, **374**, No. 2, 228 (2000).
33. L. G. Gilinskaya and Yu. N. Zanin, *J. Struct. Chem.*, **39**, No. 5, 678-686 (1998).
34. L. G. Gilinskaya, *Inorganic Materials*, **41**, No. 5, 585 (2005).

35. Ya. É. Yudovich and M. P. Ketris, *Vanadium in Coal* [in Russian], Komi Scientific Center UB RAN, Syktyvkar (2004).
36. Z. V. Bliskovskii, *Constitution and Washability of Phosphate Ores* [in Russian], Nedra, Moscow (1983).
37. V. I. Slavin and N. A. Yasamanov, *Methods of Paleogeographic Studies* [in Russian], Nedra, Moscow (1982).
38. Yu. V. Mirtov, Yu. N. Zanin, N. A. Krasilnikova, et al., *Ultramicrostructures of Phosphates* [in Russian], Nauka, Moscow (1987).
39. L. G. Gilinskaya, T. N. Grigorieva, G. N. Okuneva, and Yu. A. Vlasov, *J. Struct. Chem.*, **44**, No. 4, 622-631 (2003).
40. L. G. Gilinskaya, G. N. Okuneva, and Yu. A. Vlasov, *ibid.*, No. 5, 813-820.
41. L. G. Gilinskaya, N. A. Rudina, G. N. Okuneva, and Yu. A. Vlasov, *ibid.*, No. 6, 1038-1045.
42. I. N. Marov and N. A. Kostromina, *EPR and NMR in Chemistry of Coordination Compounds* [in Russian], Nauka, Moscow (1979).